Interfacial melting of thin ice films: An infrared study

Vlad Sadtchenko and George E. Ewing

Citation: The Journal of Chemical Physics **116**, 4686 (2002); doi: 10.1063/1.1449947
View online: http://dx.doi.org/10.1063/1.1449947
View Table of Contents: http://scitation.aip.org/content/aip/journal/jcp/116/11?ver=pdfcov
Published by the AIP Publishing

Interfacial melting of thin ice films: An infrared study

Vlad Sadtchenko[a] and George E. Ewing[b]
Department of Chemistry, Indiana University, Bloomington, Indiana 47405

(Received 15 October 2001; accepted 17 December 2001)

Interfacial melting of ice has been examined by infrared spectroscopy for the first time. Thin ice films, from 10 to 20 nm thick, were prepared on a face of a germanium prism and studied over a range of temperatures just below the triple point. Interrogation was by attenuated total reflection (ATR) spectroscopy. Interfacial melting regions were distinguished from the underlying ice by comparisons of their spectra with the well established infrared signatures of bulk water and ice. Near the triple point, e.g., $-0.15\,^{\circ}\mathrm{C}$, the spectroscopic profile of the surface melting region is indistinguishable from that of liquid water. This is compelling evidence that the commonly labeled quasi-liquid layer is indeed like liquid water. The extent of infrared extinction from ice films was used to determine the thickness of the quasi-liquid layers. At $-0.03\,^{\circ}\mathrm{C}$ the thickness is 15 nm corresponding to 40 monolayers of liquid but at $-10\,^{\circ}\mathrm{C}$ less than a monolayer remains. We compare our measurements of surface melting with those of others, sometimes finding discrepancies in thickness by two orders of magnitude. The promise of infrared spectroscopy to the further study of interfacial melting of ice is discussed. © *2002 American Institute of Physics.*
[DOI: 10.1063/1.1449947]

I. INTRODUCTION

Michael Faraday observed in 1850 ''that a particle of water which could retain the liquid state whilst touching ice on only one side, could not retain the liquid if it were touched by ice on both sides.'' [1] Thus began the concept of interfacial melting, and the presence of a liquid water film on the surface of ice at temperatures of 0 °C and below. While it was known that ''two pieces of thawing ice, if put together, adhere and become one,'' the mechanism of this refreezing (regelation) process was under debate. In 1860 Faraday reviewed the proposed mechanisms then current.[2] Some felt that it was a pressure effect since it had been established by J. Thompson and his brother W. Thompson (later Lord Kelvin) that pressure lowers the melting point of ice. Tyndall used the pressure effect to explain the flow of glaciers. Others suggested that there exists a temperature gradient through ice and, as a result, it is essentially colder in the interior than on the surface. In his typical elegant style, Faraday dispelled both the pressure and temperature arguments by a simple experiment.[2] He constructed a well-insulated chamber maintained at 0 °C by packing it with ice. Within this chamber, and in thermal contact with the ice, was a glass jar containing water. He prepared two small blocks of ice with woolen threads attached through holes near their corners. He submerged the blocks in the water by tying the threads to pieces of lead at the bottom of the jar. The ice, anchored in place by the woolen threads, assumed positions of stability due to their buoyancy. By gently moving the blocks toward each other with slips of wood, Faraday found that they adhered (''stick like leaches'') as soon as their faces touched. Thus under isothermal conditions at 0 °C and with negligible pressures regelation of ice occurred.

Interest by Faraday and others in interfacial melting, confined to understanding the properties of blocks of ice, snow or glaciers, has expanded over the last 150 years. Thin film water on ice is now implicated in the electrification of clouds[3,4] and is involved in a vast array of environmental phenomena including frost heave, soil freezing, and perma-frost.[5,6] Chemical transformation of ice crystals in polar snow pack[7] and in tropospheric and stratospheric clouds[8] affects atmospheric ozone concentrations and is an interfacial phenomena likely to involve thin film water. Ice nucleation begins at an interface with thin film water an intermediary.[9] Finally surface melting is now known to be a general phenomenon and observed in many solids of which ice is perhaps the most complicated.[10] In short, the study of interfacial melting of ice continues to be a lively research area.

The investigation of the ice interface has tended to follow technological advances. Faraday used the highest purity ice available at the time—harvested from Wenham Lake in Massachusetts, packed in sawdust, and shipped to London.[11] His cryostat was insulated with dry flannel. Both the control of cold temperatures and their measurements to the mK level can now be routinely obtained with commercial devices.[12] Some recent experiments have used synchrotron radiation sources[13] and calculations performed on supercomputers.[14] Our approach has been somewhat simpler.

Over the past few decades there have been a number of measurements of interfacial melting and it has been the subject of recent reviews.[15–17] In some studies the thickness of the thin film, variously called the quasi-liquid layer (QLL), liquidlike layer, surface melting layer, or premelting layer, has been determined. In order to put our investigation in the

[a]Present address: Department of Chemistry, George Washington University, 725 21st Street, Washington, DC 20052.
[b]Author to whom correspondence should be addressed. Electronic mail: ewingg@indiana.edu; telephone: (812) 855-5754; fax: (812) 855-8300.

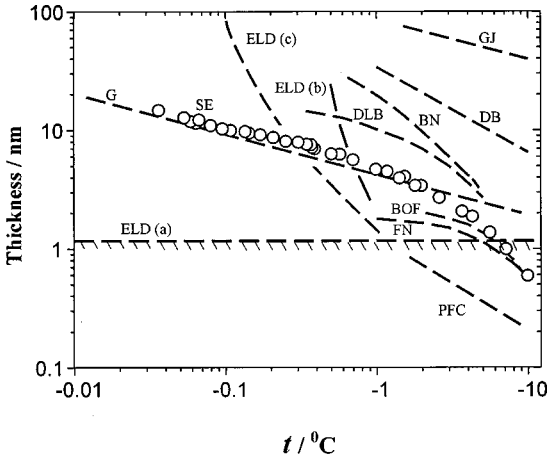

FIG. 1. Measurements of the thickness of thin film water on the ice. The studies represented are: ''ELD'' Elbaum *et al.* (Ref. 15) where (a) refers to the prism face, (b) to the basal face, and (c) to the basal face exposed to air, ''FN'' Furukawa and Nada (Ref. 22), ''BN'' Beaglehole and Nason (Ref. 21) [as analyzed by Elbaum *et al.* (Ref. 15) in their Fig. 1], ''BOF'' Bluhm *et al.* (Ref. 22), ''G'' Gilpin (Ref. 24), ''SE'' Sadtchenko and Ewing (this work), ''DLB'' Dosch *et al.* (Ref. 13), ''PFC'' Pittenger *et al.* (Ref. 20), ''DB'' Döppenscmidt and Butt (Ref. 19), and ''GJ'' Golecki and Jaccard (Ref. 18).

context of other work we have offered a sampling of thickness measurements as a function of the temperature in Fig. 1. *Caveat lector*: In order not to further overwhelm the figure and obscure trends, we have chosen not to indicate the often large error bars in any of the data represented. A variety of different techniques is represented. Proton backscattering, ''GJ,'' [18] atomic force microscopy, ''DB,'' [19] and ''PFC,'' [20] optical ellipsometry, ''BN,'' [21] grazing angle x-ray diffraction, ''DLB,'' [13] photoelectron spectroscopy, ''BOF,'' [22] molecular dynamics calculations, ''FN,'' [23] and optical reflection, ''ELD (a), (b), and (c).'' [15] A mechanical measurement involving the change in velocity of a weighted wire cutting through a block of ice as a function of the temperature is indicated by ''G.'' [24] Our study using the extinction of infrared radiation is labeled ''SE.''

To begin there are vast disagreements among the different measurements. At $-1\,^{\circ}\mathrm{C}$ for example, the thickness values range over two orders of magnitude from around 1 to 100 nm. Taking the thickness of a monolayer of liquid water to be 0.3 nm, this corresponds to 3 to 300 molecular layers. Part of the disagreement can be understood by realizing that, with the exception of the atomic force measurements and the molecular dynamics calculations, the thickness determinations are indirect and involve a web of assumptions for their deconvolution. The atomic force method is however complicated by tip perturbations.[19,20] Indeed Pittenger *et al.*[20] demonstrate a significant thin film thickness difference by treating the tip to make it hydrophobic. In the molecular dynamics calculations, the interfacial disorder due to surface melting presents a clear picture.[23,25] Perhaps too clear since classical mechanics is assumed and the intermolecular potential for water is approximate. We shall be critically evaluating some of these techniques for determining thin film water thicknesses along with our own method later in the paper.

While some of the discrepancies shown in Fig. 1 are due to the measurement methods others are due to the nature of the ice sample. Several studies[13,15,23] find differences in thickness of the thin film when interrogating the various faces (e.g., prism or basal) of a single crystal. This is emphasized in the optical reflection study where on the prism face in ''ELD(a)'' the film could not be detected (<1.2 nm) but for the basal face in ''ELD(b)'' an easily measurable thickness was reported.[15] In some experiments, including our own, a polycrystalline ice sample was used. Interfacial melting of ice against water vapor or against air gives a different thickness result. The optical reflection study for example finds thin film water on the basal face of ice in air to approach 100 nm, ''ELD(c),'' but for the same face of ice in the presence of only water vapor, films much greater than 20 nm break up into drops ''ELD(b).'' [15] Interfacial melting against the supporting substrate is also expected to affect thin film water thickness.[15] Indeed some measurements explore surface melting at the ice/vapor interface (e.g., optical ellipsometry ''ELD,'' optical reflection ''BN,'' grazing angle x-ray diffraction ''DLB,'' photoelectron spectroscopy ''BOF,'' and molecular dynamics calculations ''FN''), others interrogate an ice/substrate interface (e.g., atomic force microscopy ''PFC'' and ''DB'' or mechanical measurements ''G''). Our infrared study of thin film ice, ''SE,'' is sensitive to both interfaces and the measurement given is the sum of the two quasi-liquid thicknesses. Finally impurities in ice that will be expelled into the thin film during surface melting is predicted to alter the film thickness.[26]

Our approach to investigating interfacial melting is to grow a polycrystalline ice film on the face of a prism (in this particular study germanium) and to monitor the sample by attenuated total reflection (ATR) spectroscopy.[27]

II. EXPERIMENT

A. Overview

Schematic representations of the apparatus used for studies of interfacial melting in thin ice films are given in Fig. 2. The upper section of the figure shows the main chamber consisting of the cryogenic reservoir, transfer optics, and vacuum system. A detail of the thin film assembly is illustrated in the lower section of the figure. The ice films are grown on the bottom surface of a germanium prism that comprises one wall of a vapor chamber. Vapor is supplied to the chamber through a solenoid valve connected to a vacuum manifold and a flask of liquid water. The prism is in thermal contact through its upper surface to a cold finger at the bottom of the cryogenic reservoir. An infrared beam from a Fourier transform infrared (FTIR) spectrometer is focused into the prism to interrogate the ice film and onto a detector. The light extinction due to the presence of the thin ice film on the lower prism surface is through attenuated total reflection (ATR). We consider next in detail the individual components of this apparatus, the technique for ice film growth, and the method for the analysis of the extinction spectra of thin films by the ATR technique.

B. The prism

The substrate for the ice film is a trapezoidal germanium (Ge) prism (Reflex Analytical Corp) with all surfaces pol-

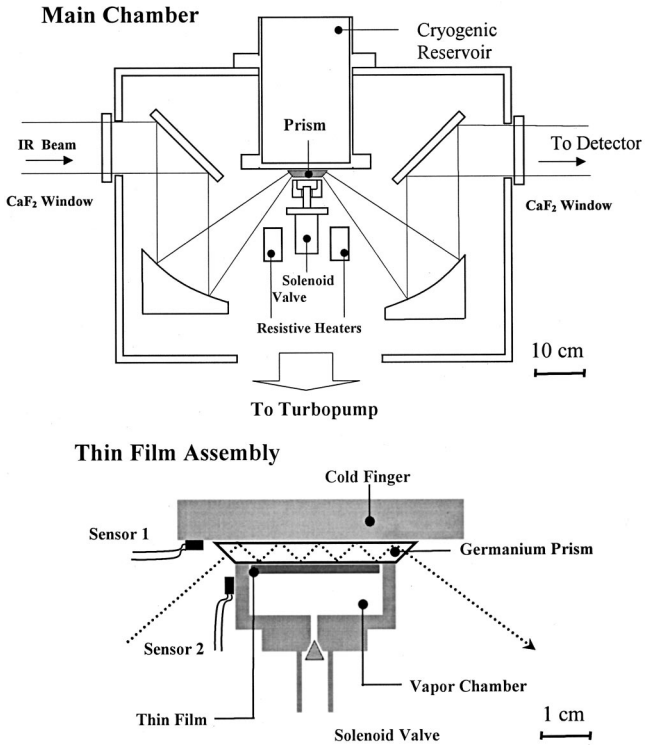

FIG. 2. Apparatus for the study of thin film ice by infrared extinction spectroscopy.

ished to $\lambda/10$. The lower surface onto which the ice film is grown is $1.2\times2.7\ \mathrm{cm}^2$. The upper surface, $1.2\times3\ \mathrm{cm}^2$, is in thermal contact with the cold finger by way of being compressed against an indium gasket. The end faces, $1.2\times0.3\ \mathrm{cm}^2$, are canted at 45° with respect to the upper surface. The dimensions of the prism end faces and upper and lower surfaces were chosen to accommodate the 7 mm focal image of the infrared beam. The angle of 45° is considerably above the 14° critical angle for germanium,[28] and was selected to assure that the prism acted in its total internal reflection mode.

The prism was used as received, the only treatment being that it was rinsed thoroughly with de-ionized water.

C. Vacuum system

The main chamber was evacuated with a turbomolecular pump (Leybold 151C), backed by a mechanical pump (Leybold D4), and combined with a liquid nitrogen cooled trap. The typical pressure of the main chamber was 10^{-6} mbar as measured by an ion gauge. The high vacuum inside the chamber served two purposes. First, it significantly reduced heat transfer from the outer walls of the main chamber to the thin film assembly and made it possible to control temperature gradients in the vapor chamber and across the prism. Second, since the prism was always colder than the body of the main chamber, the high vacuum prevented condensation of water vapor and other condensables onto its end faces. The accumulation of water or other substances here would complicate the ATR spectra of the thin film ice on the prism lower face.

The vapor chamber was pumped out and water introduced through a direct flow solenoid valve (General Valve) that could be operated either in an on/off or in a pulse mode. A pulse valve driver (General Valve Division of Parker Corp.) allowed valve openings for periods as short as 2 ms with a repetition rate up to 100 Hz.

D. Temperature control

The temperature was maintained at the lower prism face through the careful control of heat flow. In this dynamic mode, heat was removed to the cryogenic reservoir of the cold finger above the prism and supplied through resistive heaters attached to the solenoid valve below the prism. An important advantage of this cooling arrangement is that the prism is in the stream of the heat flow so that ice formation will be favored on the prism face rather than on the other walls of the vapor chamber.

The heat sink was provided by circulating the cooling fluid from a variable temperature refrigerator (Julabo FP50) through a coil immersed in ethanol contained in the cryogenic reservoir. While the temperature control of the fluid in this unit was only $\pm0.1\,^{\circ}\mathrm{C}$, the 1 kg mass of the cryogenic reservoir, constructed of stainless steel (top) and copper (bottom), assured a sluggish temperature drift easily compensated by the resistive heaters.

The two resistive heaters (8.0 Ω carbon resistors), glued to the sides of the solenoid valve, were energized by a current limited power source (Sorenson LS18-5). The heaters nominally operated at 10 W and could be controlled to ±50 mW.

The temperature in the region of the prism was continually monitored through a digital readout (Lakeshore Cryogenics Temperature Monitor 218E) by two silicon diode sensors (Lakeshore Cryogenics Silicone Diode Sensors DT-670). Sensor 1 was glued to the undersurface of the cold finger, and sensor 2 glued to a side of the vapor chamber. These sensors were calibrated by the manufacturer for ±5 mK although the overall temperature accuracy was specified to ±55 mK in the region 1 to 500 K. Nevertheless, we experimentally determined that our two sensor arrangement provided the relative temperature measurements with an accuracy on the order of $\pm0.005\,^{\circ}\mathrm{C}$ in the temperature range of our experiments -30 to $0\,^{\circ}\mathrm{C}$.

From the design of the thin film assembly and the placing of the sensors, we infer that the temperature of the lower face of the prism, and therefore the ice film, is accurate to $\pm0.005\,^{\circ}\mathrm{C}$. Using this dynamic mode of temperature control, the prism could be maintained in the range -30 to $0\,^{\circ}\mathrm{C}$ to an accuracy of $\pm0.05\,^{\circ}\mathrm{C}$ for long term (1 h) and $\pm0.005\,^{\circ}\mathrm{C}$ for short term (2 min).

E. FTIR and transfer optics

A collimated infrared beam from an FTIR spectrometer (Bruker IFS66) was introduced into the main chamber through a CaF_2 window. The beam was reflected by a plane mirror to a 45° off-axis parabolic mirror of focal length 20 cm. This focal length was chosen to be compatible with the optics of the spectrometer so that the focus diameter, near the

center of the prism, was that of the 7 mm source image. The optical arrangement was such that the infrared beam underwent a total of nine reflections, with four reflections on the lower side of the prism where the ice films were grown. Upon leaving the prism, the radiation was collected by a second parabolic mirror and transferred by a plane mirror through the exit CaF_2 window of the main chamber and onto a liquid nitrogen cooled MCT detector (Infrared Associates). All mirrors were front surface gold coated.

The main chamber was coupled to the spectrometer and detector through a Lucite box purged with dry nitrogen to reduce spectroscopic interference by atmospheric gases.

Spectra were obtained at $4\,\mathrm{cm}^{-1}$ resolution with typically 250 scans requiring about 1 min. A background spectrum was recorded for the cooled prism with signal intensity I_0 before the growth of the ice film. The signal with ice is given by I and the extinction recorded as $E=\log_{10} I_0/I$. The peak-to-peak noise level under the conditions of these experiments was typically less than 5×10^{-4}. As we shall show later this allows us to detect ice at the submonolayer level.

F. Ice film preparation

Spectrophotometric water (Johnson Matthy, Ward Hull, MA), degassed by several freeze–thaw cycles, was stored in a glass flask on a stainless steel vacuum manifold serviced by a turbopump and liquid nitrogen trap and maintained at a base pressure of 10^{-6} mbar. Filling the vapor chamber was by way of a flexible 1/4 in. thin wall stainless steel tube fitted to the bottom of the solenoid valve.

At the start of an experiment the vapor chamber, at room temperature, was pumped out through the open solenoid valve for a few hours, the valve was then closed and the temperature of the thin film assembly was brought down to 0 °C. A temperature difference of about 0.01 °C between sensor 1 and sensor 2 was created by passing a weak current through the resistive heaters so that the prism surface would be at a slightly lower temperature than the other vapor chamber walls. Water vapor was then injected into the chamber at a pressure of 10–12 mbar by opening the solenoid valve for 100–200 ms. Condensation of the water vapor on the prism resulted in the formation of a liquid water film with a typical thickness of 100 to 200 nm as verified by its ATR spectrum. The liquid film was then frozen by lowering the temperature to −28 °C. The temperature gradient introduced during film preparation did not eliminate entirely the possibility of the vapor condensation elsewhere inside the vapor chamber.

The thickness of the ice film was then decreased to 10–20 nm, as ascertained by its ATR spectrum by pumping the vapor chamber for 100 to 500 ms. After this final adjustment of the film thickness, the solenoid valve was kept closed for the duration of an experiment on a particular film.

G. Analysis of extinction spectra

The optical arrangement of the infrared radiation in the Ge prism results in total internal reflection as it undergoes its traversal. Each reflection suffers no energy loss at the prism interface while an evanescent wave penetrates beyond the clean prism surface. When this surface is host for an absorbing medium (i.e., water and/or ice) the reflection is no longer total since the evanescent wave will be attenuated. Analysis of the attenuated total reflection (ATR) signal then contains information on the thickness[29] and optical properties of the medium at the interface.[30]

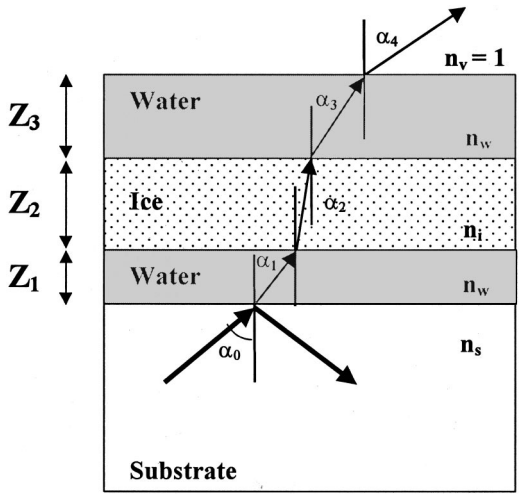

FIG. 3. Five layer model for the optical study of interfacial melting of thin film ice.

Analysis of reflection and transmission of light at interfaces and through stratified media is well established and elegantly described by Born and Wolf.[30] We model the system we are studying by considering five layers as represented schematically in Fig. 3: the semi-infinite prism substrate, a prism/ice interfacial melting region of spacing Z_1, ice of thickness Z_2, an ice/vapor interfacial melting region of spacing Z_3, and finally the semi-infinite water vapor layer. Radiation within the prism substrate, of index of refraction n_s, penetrates an interfacial melting region between germanium and ice. We model the interfacial melting region as liquid water with index of refraction n_w. Next thin film ice with index of refraction n_i is penetrated. Light escapes into another water interfacial region, also with index of refraction n_w, between ice and water vapor. Since the vapor in the uppermost layer is of low density we take its index of refraction, n_v, to be that of vacuum. The crossing of each interface is represented by a corresponding angle: α_0 to α_4 as shown in Fig. 3. The geometric arrangement of the prism with $\alpha_0 = 45°$, determines the values of α_1 to α_4. The penetration into the liquid and/or ice layers involves both reflection and absorption losses. What matters to our measurement is the fraction of light returned to the prism. If no water or ice is on the prism, the extinction will be given by $-\log(|r_0|^2)=0$ since the reflection coefficient is $r_0=1$ for total and unattenuated internal reflection. Calculation of r with the layered films present is more involved. Fortunately all the tedious algebra is laid out in matrix form[30] and amenable to programming.

Extinction calculations are carried out using Mathcad 2000 mathematical software (MathSoft Engineering and Education, Inc.). Extinctions were calculated from 1500 to $4000\,\mathrm{cm}^{-1}$ for 350 different wave number values. In all calculations the incidence angle was set at 45°, the refractive

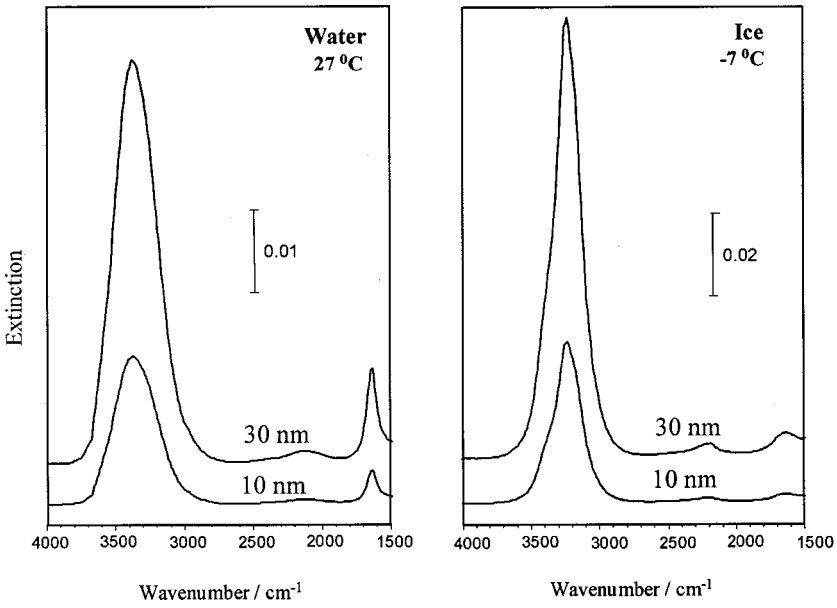

FIG. 4. Calculated infrared extinction spectra of thin film water and thin film ice.

index of Ge, $n_s = 4.00$,[28] was used for the substrate and $n_v = 1.00$ was taken for the region above the film. The optical measurements of S. G. Warren[31] at $-7\,^{\circ}\mathrm{C}$ were taken for the complex index of refraction of ice and the data of Downing and Williams[32] at $27\,^{\circ}\mathrm{C}$ for liquid water.

Sample calculations with TE polarization (electric field perpendicular to the plane of Fig. 3) serve to demonstrate the photometric potential of ATR for the study of thin films and the ability to distinguish between water and ice. First we calculate the extinction spectrum of a single film of water of thickness $Z_1 = 10$ nm. (Referring to Fig. 3, there is no ice present so $Z_2 = 0$ nm and since there is only one water film $Z_3 = 0$ nm.) The result is shown in Fig. 4. The interpretations of these bands are well established.[33,34] The most intense feature, centered near 3400 cm^{-1} is diffuse and structureless. It is associated with the ν_1, ν_3 modes of the OH stretching vibrations of H_2O within the hydrogen bonding network of the liquid. The somewhat sharper feature near 1650 cm^{-1} is assigned to the ν_2 bending mode. Finally the weak feature near 2200 cm^{-1} is associated with a combination band. The water extinction spectrum at $Z_1 = 30$ nm is shown for comparison. Although the overall profiles for the two thickness are similar, their extinctions do not scale linearly. A threefold increase in the extinction of the 10 nm spectrum would extrapolate to 0.052 while the calculated result at 0.047 is noticeably less (9% difference). While there is close to linear ($<3\%$) response of extinction to thicknesses below 10 nm the deviations become noticeable above 20 nm. The interpretation of the nonlinear extinction response has to do with the limits of the penetration of the evanescent wave into the absorbing film and is discussed in detail by Zhang and Ewing.[29]

The calculated extinction spectrum of ice at 10 nm is also shown in Fig. 4 for comparison. It is distinct from the spectrum of water for the same thickness in a number of respects. The region of the OH stretching vibration is red shifted to 3200 cm^{-1}, the bandwidth is considerably narrower and its profile reveals structure through a shoulder on its high wave number side, and finally its maximum extinction is double that of water. The ν_2 region of ice, by contrast, is both weaker and more diffuse than that of the liquid. All these spectroscopic differences have been interpreted qualitatively in terms of the changes of the hydrogen bonding network of the H_2O molecules on the phase change from liquid to solid.[33,34]

As in the case of the calculated spectrum of water, the extinction of ice shows a close to linear response with thicknesses below 15 nm. The calculated extinction for 0.37 nm (corresponding to a single bilayer of I_h ice[16]) of 1.4×10^{-3} exceeds our noise level of 5×10^{-4} allowing a signal to noise ratio of 3. Thus the spectroscopic technique we have chosen allows, in principle, the study of thin films of ice into the submonolayer level.

III. RESULTS AND DISCUSSION

A. The germanium surface

Since the Ge prism surface on which thin films of ice were successfully grown was undefined, we can only speculate on its properties. It was polished from an unoriented single crystal of germanium. We anticipate that the particles of the polishing grit left the surface scored. Moreover the dangling bonds of the Ge atoms at the surface as well as those on the edge and corners produced by the polishing process are prone to oxidation.[35] We are left with a surface that is neither smooth on an atomic scale nor chemically specified and on a microscopic scale only flat to $\lambda/10$ ($\sim$60 nm) yet can accommodate ice films of $\sim$10 nm thickness. The irregular Ge surface as a platform for ice growth is in marked contrast to the presentation of the $BaF_2(100)$ face. This well defined and atomically smooth ionic surface has a lattice constant that matches within a few percent of that of the basal face of I_h,[36] yet fails to support a stable ice film.[37] We shall explore this paradox in a later paper. For the convoluted Ge face, rather than having its valleys and depressions filled in to produce an ice coating of variable thickness,

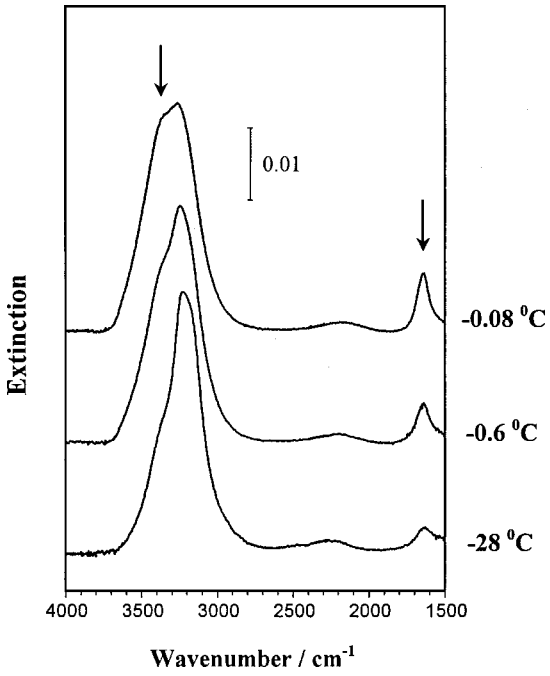

FIG. 5. The growth of interfacial melting layers on thin film ice.

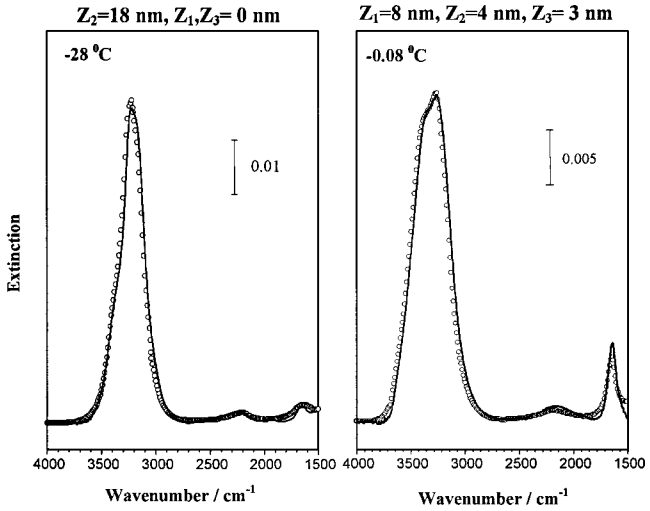

FIG. 6. Comparisons of calculated (open circles) and measured extinction (solid lines) spectra of thin film ice. At $-28\,^{\circ}\mathrm{C}$ there is not interfacial melting. At $-0.08\,^{\circ}\mathrm{C}$ there is interfacial melting.

a uniform film apparently accommodates the surface contours. This proposed morphology of thin film ice on Ge is borne out by the spectroscopy and our desorption experiments to be presented below.

B. Ice film extinction spectra

Figure 5 shows the spectra of thin ice films at several temperatures. We began by preparing an ice film 10–20 nm thick at $-28\,^{\circ}\mathrm{C}$. This film was warmed gradually from $-28\,^{\circ}\mathrm{C}$ to $-0.03\,^{\circ}\mathrm{C}$ and the film spectra were measured at various temperatures. Typical rate of temperature change was on the order of $0.1\,^{\circ}\mathrm{C}$/min at temperatures below $-15\,^{\circ}\mathrm{C}$, about $0.05\,^{\circ}\mathrm{C}$/min at temperatures from $-15\,^{\circ}\mathrm{C}$ to $-3\,^{\circ}\mathrm{C}$, and less than $0.005\,^{\circ}\mathrm{C}$/min at temperatures from $-3\,^{\circ}\mathrm{C}$ to $0\,^{\circ}\mathrm{C}$. Thus, the typical time, required to obtain spectral measurements in the temperature range from $-28\,^{\circ}\mathrm{C}$ to near $0\,^{\circ}\mathrm{C}$, was 10–12 h.

As determined by analysis, which we will describe in detail in the following sections, the overall thickness of the film typically fluctuated by as much as 2 nm, from one spectrum measurement to another (taken every 15 min). Furthermore, the average thickness could drift during warming from -28 to $0.03\,^{\circ}\mathrm{C}$ by as much 7 nm. However, the fluctuations, and long-term drift in the film thickness were always less than 0.13 nm/min. (This corresponds to less than an half bilayer of ice during the time it takes to record a spectrum.)

Adding water vapor through the solenoid valve to compensate for thickness fluctuations was avoided during all experiments to prevent the possibility of creating a mixture of supercooled water and ice on the Ge surface. However, on a few occasions, the film was pulse-pumped to reduce the film thickness by 3–5 nm.

A cursory comparison of the Fig. 5 spectrum at $-28\,^{\circ}\mathrm{C}$ with Fig. 4 shows that it has the signature of ice. Both calculated and observed extinction spectra reveal a strong feature near $3200\ \mathrm{cm}^{-1}$ with a shoulder on the high wave number side and a less prominent diffuse feature near $1650\ \mathrm{cm}^{-1}$. As the film temperature is increased toward $-10\,^{\circ}\mathrm{C}$, the spectroscopic signature (not shown) is essentially unchanged. Subtle changes occur on closer approach to the ice melting (triple) point. At $-0.6\,^{\circ}\mathrm{C}$, a distinct shoulder (indicated by the arrow) has formed near $3400\ \mathrm{cm}^{-1}$ and the extinction near the bending mode (indicated by the arrow) has sharpened. At $-0.08\,^{\circ}\mathrm{C}$ the $3400\ \mathrm{cm}^{-1}$ shoulder extinction is comparable to that of the band center near $3200\ \mathrm{cm}^{-1}$. Finally the extinction in the bending mode region has both increased and sharpened. Reference to Fig. 4 suggests the presence of a liquid component in the thin ice film. We have then qualitative evidence for interfacial melting of ice as it approaches its triple point. We can make this interpretation quantitative by attending to the details of the ATR spectroscopic analysis of thin films on a Ge prism substrate as described in the previous section.

Calculations were performed for both TE and TM polarizations. The infrared beam polarization and thicknesses of the three layers Z_1, Z_2, Z_3 were varied to produce the optimum fit of the observed extinction spectra. The best fit of the data was always obtained at 90% TE polarization. While the incoming infrared radiation from the FTIR was not intentionally polarized, it became largely TE polarized by the nine multiple reflections within the Ge prism with its large index of refraction. While geometric considerations and Fig. 2 suggest four reflections against the absorbing face of the prism, there is a spread in the focused infrared beam rather than its being parallel. In a separate experiment we have empirically determined that the effective number of reflections was 3.5 rather than 4. We have therefore used 3.5 reflections in all the extinction spectra calculations.

Extinction calculations (given by the open circles) for the thin ice film at $-28\,^{\circ}\mathrm{C}$ are compared with the observed spectrum (the solid line) in Fig. 6. In the calculated optimization of the layer thicknesses, we have found an ice film

thickness, Z_2, = 18 nm, and no contribution from interfacial water, Z_1, Z_3 = 0 nm. The agreement is excellent.

Extinction analysis of the thin film at −0.08 °C finds the ice of thickness Z_2 = 4 nm but requires interfacial water. This water can be partitioned as Z_1 = 8 nm and Z_3 = 3 nm as we indicate in Fig. 6 or in any combination for the two interfacial melting layers as long as $Z_1 + Z_3$ = 11 nm. Again the agreement is excellent. The agreement is surprising considering the simplifying assumptions needed for the calculation: The interfaces are assumed smooth on a nanometer scale, and the optical constants of the ice or water films are those of the bulk material.

The close match of the calculated extinction spectra with the observed spectra in Fig. 6 is a strong conformation of the three-layer water/ice/water model introduced in Fig. 3 and shows that the spectral changes can be explained by interfacial melting.

For simplicity in notation, and in keeping with tradition,[16] we shall call a interfacial melting region the quasi-liquid layer or QLL. There are two such layers. One between ice and the substrate we call QLL_{is} and one between ice and vapor we call QLL_{iv}. By reducing the temperature of thin film ice we also reduce the thickness of their sum: $QLL_{is} + QLL_{iv}$. In the following experiment we explore in detail the spectra of the quasi-liquid layers.

C. QLL spectra

Encouraged by the successful analysis of Fig. 6 we proceed to extract the QLL spectra from the spectroscopic profiles of ice films. We know from Fig. 6 that there is a negligible QLL at −28 °C and the profile is quantitatively modeled using the optical constants of bulk ice. Since the ATR spectra are likely sums of the quasi-liquid layers and ice it is possible to determine the total QLL thickness by subtracting the ice film extinction spectrum from the overall thin film extinction spectrum. This simple recipe is: spectrum of $QLL_{is} + QLL_{iv}$ = (overall spectrum) $= -C$ (spectrum of ice) where C is an adjustable scaling parameter. The results of this subtraction for several temperatures approaching the triple point are shown in Fig. 7.

When the ice film temperature is close to the triple point, the liquid layer is thick and the $QLL_{is} + QLL_{iv}$ spectroscopic signature is indistinguishable from bulk water. This is illustrated in Fig. 7 at −0.15 °C. The solid line is the result of the subtraction procedure and the open circles the result of the extinction spectrum calculation using bulk water optical constants. *That the spectroscopic profiles for bulk liquid water and the ice surface melting region are in excellent agreement over their entire extinction range, 2800 to 3800 cm^{-1}, is compelling evidence that the quasi-liquid layer is indeed like liquid water*. At −0.15 °C the thickness of the quasi-liquid layers is $Z_1 + Z_3$ = 9 nm. As the ice film gets colder, i.e., −1.0 °C, the liquid film band center shifts away of that expected for bulk water. At −3.2 °C with $Z_1 + Z_3$ = 2 nm the band center is now 3300 cm^{-1}. Using the density of liquid water at 0 °C,[38] we can estimate an average molecular layer of 0.31 nm. Thus a liquid film of 2 nm would correspond to seven molecular layers. If this is partitioned between QLL_{is} and QLL_{iv} it is perhaps not surprising to find a deviation from bulk water behavior.

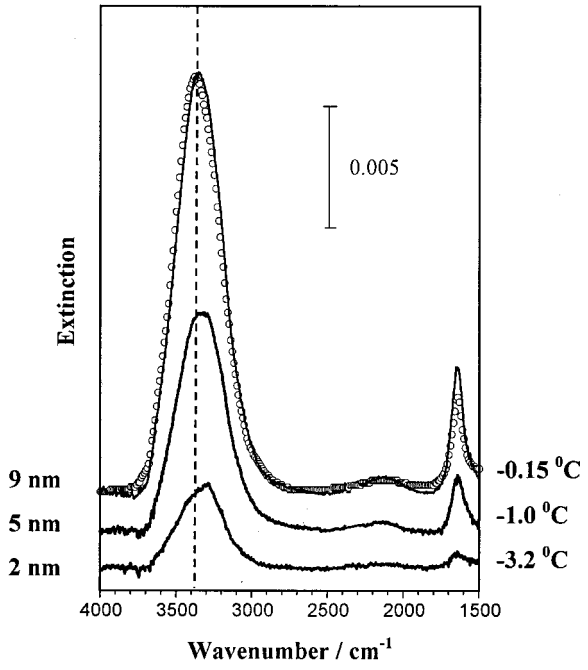

FIG. 7. Spectra of the quasi-liquid layer (QLL) on ice films. The QLL thicknesses are shown on the left side of the figure. Near the triple point, −0.15 °C, for the 9 nm QLL the observed extinction spectrum (solid line) is indistinguishable from the calculated spectrum (open circles) using bulk liquid water optical constants. Far from the triple point (−3.2 °C), the 2 nm film extinction spectrum exhibits a profile that differs from the bulk spectrum.

Several important conclusions follow from these observations. At temperatures in the range −1 °C to 0 °C, the properties of the quasi-liquid layers appear close to liquid water. We can then expect the estimation of the liquid thickness to be reliable. At temperatures below −1 °C, the distorted bandshape suggests that liquid film properties, because of its thinness, to be different from those of bulk water. Estimates of liquid thickness below 2 nm cannot be expected to be reliable. These conclusions on the similarity of the properties of the quasi-liquid layer and bulk water based on spectroscopy, are consistent with recent measurements of the viscosity of films of water greater than 2 nm by Raviv *et al.*[39]

Another uncertainty in estimation of QLL thickness needs to be addressed. During spectra subtraction we have assumed that the ATR spectra of the ice films are independent of thickness. At one extreme this cannot be true. Our previous work with H_2O on $BaF_2(111)$[36] and the work of Devlin *et al.*[40] on ice nanoparticles have demonstrated that an ice bilayer at an interface has a spectrum in the region of the OH stretching vibration different from bulk ice. However, in (unpublished) measurements of 2 nm of thin film ice on Ge at −28 °C, spectra show good agreement with that calculated assuming bulk ice optical constants. This sets a lower limit on the estimation of ice thickness of say ~1 nm. Since the bilayer spacing of I_h ice is 0.37 nm,[16] this would correspond to about three bilayers.

D. Film morphology

All our extinction spectra calculations have assumed a film morphology like that represented in Fig. 3. That is, the films are imagined smooth and uniform with premelting occurring only at planar ice/vapor and ice/substrate interfaces. In fact, the film morphology may be quite different. For example, ice on Ge might be in the form of irregular crystallites or perhaps dendritic. Alternatively ice or supercooled water could pool in depressions of the uneven Ge surface. Furthermore, even if a continuous ice film is formed, it is likely to be polycrystalline. Thus premelting may occur not only on the ice/vapor and ice/substrate interfaces but also at the grain boundaries and at triple junctions (boundaries between three grains), i.e., in the interior of the film.[16,41] Such a film would consist of inclusions of liquid water within the ice and may nevertheless give rise to the spectra similar to those shown in Fig. 5.

Even an assembly of supercooled liquid drops and ice islands may result in an ATR spectra similar to that of a smooth film, if the average size of the clusters is small. Several processes may result in such mixed structures. For example, supercooled liquid drops could form on germanium during film thickness fluctuations as a result of vapor condensation at temperatures sufficiently close to the triple point. In order to elucidate the film morphology we investigated isothermal desorption of the ice film at temperatures where extensive premelting is evident.

The desorption experiments where conducted in the following sequences: (1) The film of initial overall thickness of ~ 20 nm, maintained at constant temperature ($-0.6\,^{\circ}$C), was exposed to vacuum by opening the solenoid valve for 10 to 15 ms intervals. As a result, 3%–5% of the film evaporated. (2) After a delay of several minutes, an ATR spectrum of the film was recorded. (3) Sequences (1)–(2) were repeated until the thickness of the film was reduced by at least 70%.

A few selected spectra with the corresponding desorption times are shown in Fig. 8. Several important changes in these spectra are evident. The band shape in the $4000-2500\ \mathrm{cm}^{-1}$ wave number region is clearly altered as a function of overall film thickness. At the beginning of the desorption process, 0 ms, the spectrum of the film bears a resemblance to that of bulk ice. At 34 and 54 ms, however, the spectra are clearly developing a liquid film component. The fact that the various spectra do not scale with thickness implies that the amounts ice and liquid in the film change unequally during desorption.

Figure 9 illustrates the result of the analysis used to deconvolute the spectra obtained during desorption. In order to obtain quantitative estimates of $\mathrm{QLL}_{is}+\mathrm{QLL}_{iv}$ and ice fractions of the film we fit each of the spectra with a linear combination of *model* QLL and ice spectroscopic profiles.

The model QLL and ice spectra were produced as follows:

(1) The experimental QLL spectrum was extracted from the overall spectrum of the thickest film obtained at $-0.6\,^{\circ}$C by subtracting an ice spectrum obtained at $-28\,^{\circ}$C. The resulting experimental QLL spectrum was similar to but not identical to the bulk water spectrum.
(2) The experimental QLL spectrum was fit with a sum of four Gaussians with arbitrarily set frequencies (3200, 3300, 3400, and 3500 cm^{-1}). The widths and the heights were varied until the best fit was obtained.

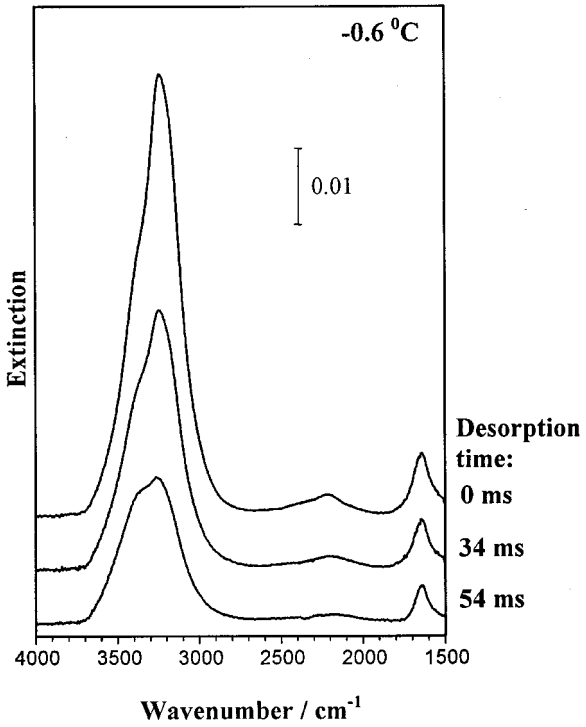

FIG. 8. Extinction spectra of an ice film as it undergoes thinning by desorption.

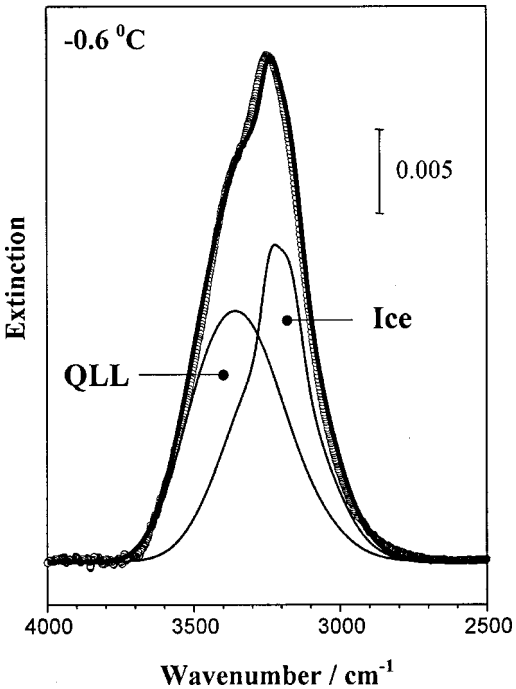

FIG. 9. Deconvolution of the extinction spectra of an ice film into its ice and quasi-liquid layer (QLL) components.

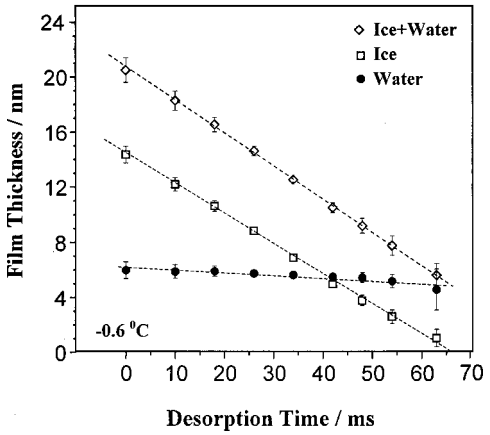

FIG. 10. Film thickness during desorption: Total thickness, ice+water (diamonds); ice thickness (squares); and water, i.e., QLL (closed circles).

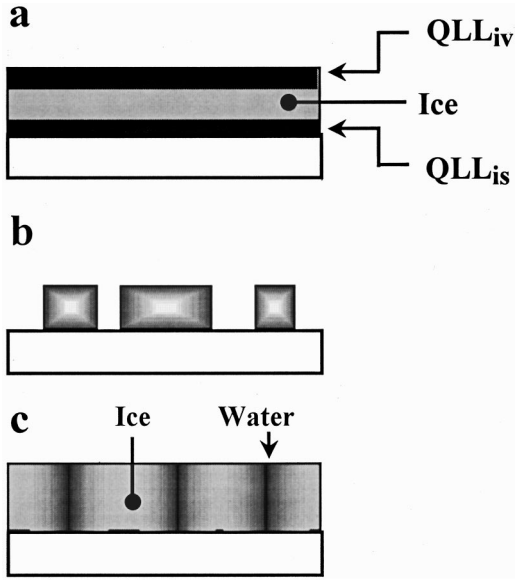

FIG. 11. Possible thin film ice morphologies. (a) Homogeneous thin film ice with a quasi-liquid layer at the ice-vapor interface (QLL_{iv}) and a quasi-liquid layer at the ice-substrate interface (QLL_{is}). (b) Crystallites of ice on the substrate. (c) An ice film with quasi-liquid located in grain boundaries.

(3) The model QLL spectrum was defined as the sum of these four Gaussians multiplied by a coefficient. This coefficient was used as the parameter during fitting of overall film spectra. Thus the model QLL spectrum is a function of one variable (wave number), and has one parameter, that adjusts its height (extinction).
(4) A similar procedure was used to obtain the model ice spectrum. Again, a sum of four Gaussians was used to fit an experimental ice spectrum obtained at $-28\,^{\circ}\mathrm{C}$. The model ice spectrum was defined as the sum of the Gaussians multiplied by a coefficient, that adjusted its magnitude, and that was used as a parameter for fitting the overall film spectra.

The spectra obtained as the result of this fitting procedure, together with the optical constants of bulk water or ice, were integrated in the wave number range from 4000 to 2500 cm^{-1} to estimate the amounts of ice and water in the film. The results are shown in Fig. 10. No assumptions about film morphology have been made at this point, however, for the sake of convenience, the water and ice contents of the film were expressed in nm, as if the film is composed of two thin layers (ice and water).

The evaporation of the film follows zero order kinetics, since the number of molecules on the substrate decreases linearly with desorption time independent of the total film thickness. It is evident that the film loss is entirely due to the decrease in the ice component since while the liquid content of the film is constant, the ice film thickness decreases by an order of magnitude. The removal of molecules from the film is accompanied by a wasting of the ice layer to feed the interfacial melting regions so that their thicknesses are maintained. Several observations about film morphology can be inferred from these results.

First of all we need to emphasize that the observed zero order kinetics is inconsistent with ice film build up in depressions on the presumably uneven Ge surface. Zero order desorption kinetics ultimately means that the net geometrical area of the ice/vacuum interface does not change with the amount of ice on the surface. Even though the ice could completely cover the extrusions and indents on the substrate at the beginning of the desorption process, the removal of ice layers would eventually result in breaking of such film into separated ice pockets. From this moment on the net area of ice/vacuum interface must begin to decrease, and the desorption kinetics must change. Such a change in desorption kinetics must be evident as soon as the *average* thickness of the ice film becomes comparable with the scale of Ge surface roughness, i.e., when the *average* ice film thickness becomes significantly less than 60 nm. Since we observe zero order desorption kinetics for films as thin as 2 nm, we are left with two possibilities. First, the Ge surface is much smoother than expected (roughness scale is significantly less than 2 nm). Second, as we speculated earlier, rather than having its valleys and depressions filled in to produce an ice coating of variable thickness, a uniform film apparently accommodates the surface contours. The combination of these two possibilities may describe the most likely Ge surface morphology, i.e., Ge prism is microscopically smooth (on the scale of 2 nm at least) but may have *gradual* thickness variation of about 60 nm.

The adlayers grown on Ge substrate under conditions present in our experiments are consistent with the smooth, continuous, thin films as shown on Fig. 11(a) and previously assumed in Fig. 3. By contrast, an alternative morphology shown in Fig. 11(b) is not consistent with observed zero order desorption kinetics, since the desorption of clusters would lead to gradual decrease in their sizes, this would result in a nonlinear decrease in their surface areas. Being proportional to the effective surface area of the condensed phase, the desorption rate would change significantly with the size of the clusters. The decrease in the desorption rate due to decrease in effective surface area of the film would be balanced to a certain extent by an increase in the vapor pressure of the clusters due to their increased curvature through the Kelvin effect.[42] However, such compensation would be

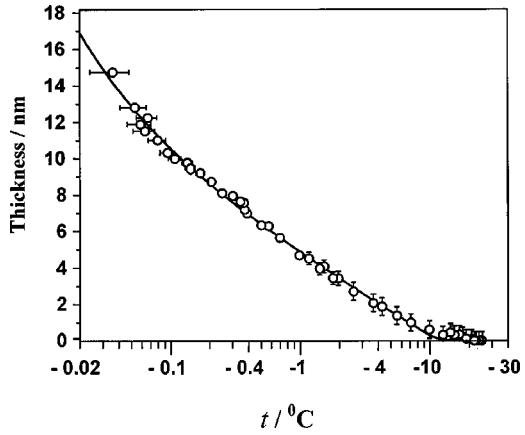

FIG. 12. Quasi-liquid layer thickness (QLL) as a function of temperature.

sensitive to temperature. That such a fortuitous balance is not the explanation, is supported by our observation (not shown here) of zero order kinetics at $-1\,^{\circ}\mathrm{C}$.

Another possible morphology, illustrated in Fig. 11(c) represents liquid inclusions or grain boundaries in the ice film. This morphology is inconsistent with the observed independence of liquid content on overall film thickness. This does not necessarily mean that premelting does not occur at the grain boundaries, which are likely present in our film. The failure to observe dependence of the liquid content on the overall thickness of the film may simply mean that the abundance of grain boundaries is low.

In our approach we interrogate QLL formation on nanometer scale films of ice. This raises concern that, the microscopic physical dimensions of our ice samples may affect the mechanisms of premelting, i.e., dynamics and mechanism of surface premelting of large ice samples used in the many past experiments can be quite different. Our experimental results, however, exclude this possibility. Indeed, as we demonstrated in this section, the change in the ice thickness by as much as 10 times does not affect significantly the QLL thickness at $-0.6\,^{\circ}\mathrm{C}$. Furthermore in a separate set of experiments, not reproduced here, we determined that doubling the ice film thickness produced QLL thickness dependence on temperature identical to the one depicted in Fig. 12. Thus we arrive to the conclusion that the physics of the interfacial premelting does not depend on the ice thickness under conditions present in our experiments. Therefore, QLL properties on a nanometer scale ice film are unlikely to differ from those on macroscopic ice samples.

E. Temperature dependence of QLL thicknesses

Having established the likely film morphology represented in Fig. 11(a) (and Fig. 3), we are ready to present the final analysis of our thin ice film spectra to arrive at the dependence of the QLL thicknesses on temperature.

In order to calculate the total or net QLL thickness at each particular temperature we adopted a procedure identical to that used for extracting water and ice fractions in the desorption experiment. Each of the measured spectra was fit with a linear combination of model ice spectrum and model QLL spectrum. The model QLL and ice spectra were defined as described in the previous section with one exception. Two additional parameters were introduced into the equation, which described the QLL functional form. The first one made possible small variations of the bandwidth, and the second adjusted the band position slightly. This was done to partially compensate deviations of the QLL spectra from neat water spectra at temperatures below $-1\,^{\circ}\mathrm{C}$. The liquid and ice spectra obtained as the result of this fitting procedure were integrated in wave number range from 4000 to 2500 cm^{-1} to estimate the net QLL thickness, the ice thickness, and overall thickness of the film. Optical constants of bulk water and bulk ice were again used to calculate these film thicknesses.

The result of this analysis is shown in Fig. 12 as the total QLL thickness dependence on temperature. The horizontal error bars represent the uncertainty in temperature measurement and the vertical error bars are due to uncertainties in the optical constants of the thin films.

Figure 12 is rich in information. We note first that the liquid film disappears below about $-10\,^{\circ}\mathrm{C}$. By disappear we mean that the contribution of the liquid component to the overall extinction spectrum below $-10\,^{\circ}\mathrm{C}$ corresponds to a thickness of less than 0.3 nm or about one monolayer of liquid water. At the high temperature limit of our measurement, $-0.03\,^{\circ}\mathrm{C}$, this thickness, 15 nm, corresponds to about 40 monolayers. We note that in this semi-logarithmic presentation, the temperature dependence of growth in the liquid film thickness is slightly bowed but changes more abruptly at the ends of the curve. When this data is plotted logarithmically for both temperature and thickness, as in Fig. 1, deviation from linearity is only apparent below $-1\,^{\circ}\mathrm{C}$ at the disappearance of the surface melting layers.

Recent theoretical investigations by Wettlaufer[26] suggest that even a very small amount of impurities will have a dramatic affect on thickness formed on ice/vapor as well as on ice/substrate interfaces. The changes in temperature dependence of QLL thickness may be very complex depending on the concentration of the impurities. For example, it was predicted that at certain temperatures adding small amount of impurities may result in *decrease* in the QLL thickness. Under conditions present in our experiments, impurities are likely to be present in the films. It is difficult to characterize quantitatively the level of contamination of our samples. However, it is likely to be relatively low. Indeed, as predicted by Wettlaufer, at high impurity concentrations the QLL dependence on temperature is proportional to $\sim T^{-1}$.[26] The QLL thickness measurements shown in Fig. 12 are clearly not in accord with this power law. Furthermore, the fact that the QLL thickness does not depend significantly on overall film thickness also indicate that the level of contamination of our ice samples is low. Though not abundant, and hard to detect, grain boundaries must be present in the bulk of our films. Thus reducing the overall thickness of the film will result in some increase in the concentration of the ionic impurities on the ice surface. If the initial concentration of the impurities is high, the change in overall thickness must result in significant change in the QLL thickness due to its predicted sensitivity of even the smallest amount of impurities.

Quasi-liquid layer properties at ice/substrate interface

are expected to be different from those at ice/vapor interface.[43] Thus the overall QLL thickness, i.e., QLL_{is} and QLL_{iv}, dependence on temperature is expected to demonstrate a complex behavior different from that observed in experiments that interrogated a single interface. Unfortunately our experiments have not been able to separately determine QLL_{is} and QLL_{iv}, only their sum. We shall discuss how this might be done in a following section.

F. Investigations of surface melting: Some comparisons

We have demonstrated surface melting of ice by infrared spectroscopy for the first time. Moreover we have been able to provide quantitative measurements of the thicknesses of the quasi-liquid layers. However, since we cannot distinguish surface melting at the ice-substrate interface from the ice-vapor interface our measurement of QLL provides only an upper limit of either QLL_{is} or QLL_{iv}.

Returning to Fig. 1, how does our data, labeled ''SE,'' compare with those of others? A thorough comparison of various experimental and theoretical approaches requires a critical examination of the assumptions needed to extract QLL_{is} or QLL_{iv} from the principle measurement. Critical reviews of some of the methods have been provided, for example by Elbaum *et al.*,[15] Dash *et al.*,[5] and in Chapter 10 of *Physics of Ice*.[16] There is unfortunately no ruler from which one can read off a liquid layer thickness. Convoluted analyses involving a web of assumptions are needed in all cases to extract a thickness from the raw data. We have taken care throughout this paper to expose the assumptions we have used to provide our values of QLL thicknesses.

In our discussion of Fig. 1 we shall offer only two comparisons of our measurements with that of others. In the case of Gilpin's[23] results, labeled ''G,'' agreement with our data *appears* remarkably good. By contrast in the comparison with the work Golecki and Jaccard.[18] labeled ''GJ,'' there *appears* to be great disagreement.

Gilpin studied the interface between the metallic surface of a tungsten wire as it slices through an ice sample. The wire velocity is limited by the viscosity of the thin film assumed to have the value of bulk supercooled water. The liquid layer thickness, at a fixed temperature, is then obtained from the velocity by way of a simple calculation involving the force on the wire and its diameter. These determinations then provide values of QLL_{is} only. In our experiment, QLL (QLL_{is} plus QLL_{iv}) is extracted from infrared extinction measurements assuming the bulk value of the complex index refraction of liquid water at 27 °C. If we were to accept all the assumptions in both methods for obtaining film thickness, the agreement would further require that we equate QLL_{is} (with ''*s*'' a metal) from Gilpin's measurements with QLL_{is} plus QLL_{iv} (with ''*s*'' *a* semiconductor), in our measurements. The agreement between the ''SE'' and ''G'' values on Fig. 1 may be fortuitous. A closer examination of the assumptions that bulk liquid values for either the viscosity or the index of refraction are acceptable approximations for thin films of water is necessary.

At the other extreme in Fig. 1 is the discrepancy between our results and the proton back scattering measurements labeled ''GJ.'' Golecki and Jaccard[18] did not actually claim to measure a liquid film thickness but rather the depth of the amorphous region near the ice surface due to molecular disorder of the water molecules. It is this disorder that disrupts the channels connecting the interior of ice to its basal face and enhance the back scatter of the probing protons. In the ''GJ'' interpretation no liquid layer need be invoked to understand the observed back scatter. A liquidlike thin film could, but need not, provide the necessary amorphous surface region. Their measurement thus provide an upper limit to QLL_{iv} values and do not necessary contradict our results for $QLL_{iv} + QLL_{is}$.

G. The infrared extinction method

We view the infrared extinction ATR method for measuring ice interfacial phenomena presented in this paper as the first demonstration of a powerful technique that has the potential for great improvement. To begin, the photometric sensitivity can be extended by probably an order of magnitude by an increased number of reflections still using a black body source[44] or by cavity ring down measurements with tunable laser excitation.[45] Different prism substrates or surface modifications would allow the growth of oriented single crystals of ice. Ice samples of different thicknesses, and analysis making use of the nonlinear extinction response illustrated in Fig. 3 and discussed elsewhere,[29] will allow distinguishing and characterizing both QLL interfaces.

The chemical and physical properties of the ice-vapor interface can be monitored with the introduction of atmospherically interesting gases (e.g., HNO_3, SO_2, HCl, CO_2, etc.) into a vapor chamber such as that shown in Fig. 2. Both the thickness of this quasi-liquid layer and its chemical transformation can be monitored by infrared extinction spectra.

Many methods for the study of surface melting at a given temperature rely on only a *single* datum. For optical measurements in the visible region it is the magnitude of the reflected light[15] or its degree of polarization.[21] In Gilpin's study[13] it is the velocity of the wire cutting through the ice. For x-ray grazing angle measurements it is the bandwidth.[13] For proton backscattering it is the fraction of returning particles.[18] A tip deflection is the outcome of ATM studies[19] with additional attention to the velocity of tip penetration.[20] Optical absorption measurements potentially contain information throughout a spectroscopic profile. This has been utilized to only a limited extent in photoelectron measurements[22] but more completely in our own study here.

In the preceding infrared analysis we have made qualitative use of bandcenters to decide two possibilities: Is the thin film quasi-liquid or solid? Following this decision band areas are used to extract a film thickness. However, as our analysis of the QLL spectroscopic profiles in Fig. 9 showed, the band shapes do not match those of the bulk samples for the thinner liquidlike layers. To avoid trying to understand these thin film spectroscopic profiles is to throw away information. As Rice *et al.* showed two decades ago,[46] and in current collaborations of Devlin and Buch,[40] the ice spectroscopic profiles can be deconvoluted to reveal the nature of the hydrogen bonding networks. The fit of a Gaussian (or some other functional form) to a spectroscopic band contains

three pieces of information: bandcenter, bandwidth and bandheight. The four Gaussians we have used to fit the QLL that contain 12 pieces of information potentially available for interpretation of the structure and dynamics of the thin film. Improved photometry will increase the information available.

Future partnerships between theory and experiments will expand our knowledge of surface melting greatly.

ACKNOWLEDGMENTS

Discussions with Zhenfeng Zhang on the analysis of thin films have been of great importance to this investigation. In addition his demonstration that germanium was a useful surface for ice growth lead the authors to choose this material for their prism. The authors are fortunate to have received comments from Professors J. G. Dash, S. C. Fain, Jr., J. S. Wettlaufer, and A. V. Rempel of the University of Washington, Department of Physics, who have closely read the manuscript. The authors have incorporated many of their suggestions in the revised paper. Peter Conrad is acknowledged for his participation in these experiments. The National Science Foundation has provided support through NSF CHE-9816299.

[1] M. Faraday, Royal Institution Discourse, June 7, 1850; *Experimental Researches in Chemistry and Physics* (Taylor and Francis, New York, 1991).
[2] M. Faraday, Proc. R. Soc. London **10**, 152 (1860).
[3] G. J. Turner and C. Stow, Philos. Mag. A **49**, L25 (1984).
[4] J. G. Dash, B. L. Mason, and J. S. Wettlaufer J. Geophys. Res. **106**, 20395 (2001).
[5] J. G. Dash, H.-Y. Fu, and J. S. Wettlaufer, Rep. Prog. Phys. **58**, 115 (1995).
[6] J. S. Wettlaufer, Philos. Trans. R. Soc. London, Ser. A **357**, 3403 (1999).
[7] B. Riley, J. Walega, D. Montzka *et al.*, J. Atmos. Chem. **36**, 1 (2000).
[8] M. J. Molina, in *Chemistry of the Atmosphere: Its Impact on Global Change*, edited by J. G. Calvert (Blackwell, Oxford, 1994), pp. 27–38.
[9] D. W. Oxtoby, in *Ice Physics and the Natural Environment*, edited by J. S. Wettlaufer, J. G. Dash and N. Untersteiner, NATO ASI Series I, Vol. 56 (Springer, New York, 1999), pp. 23–38.
[10] J. G. Dash, Rev. Mod. Phys. **71**, 1737 (1999).
[11] T. Shachtman, *Absolute Zero and the Conquest of Cold* (Houghton Mifflin, New York, 1999).
[12] *Temperature Measurement and Control* (www.Lakeshore.com)
[13] H. Dosch, A. Lied, and J. Bilgram, Surf. Sci. **366**, 43 (1996).
[14] E. R. Batista, S. S. Xanthras, and H. Jónsson, J. Chem. Phys. **112**, 3285 (2000).
[15] M. Elbaum, S. G. Lipson, and J. G. Dash, J. Cryst. Growth **129**, 491 (1993).
[16] V. F. Petrenko and R. W. Whitworth, *Physics of Ice* (Oxford University Press, Oxford, 1999).
[17] J. G. Dash, in *Ice Physics and the Natural Environment*, edited J. S. Wettlaufer, J. G. Dash and N. Untersteiner, NATO ASI Series I, Vol. 56 (Springer, New York, 1999), pp. 11–22.
[18] I. Golecki and C. Jaccard, J. Phys. C **11**, 4229 (1978)
[19] A. Döppenscmidt and H.-J. Butt, Langmuir **16**, 6709 (2000).
[20] G. Pittenger, S. C. Fain, Jr., M. T. Cochran, J. M. K. Donev, B. E. Robertson, A. Szuchmacher, and R. M. Overney, Phys. Rev. B **63**, 134102 (2001).
[21] D. Beaglehole and D. Nason, Surf. Sci. **96**, 363 (1980).
[22] H. Bluhm, D. F. Ogletree, C. S. Fadley, M. Salmeron, and Z. Hussain, J. Phys. B (submitted).
[23] Y. Furukawa and H. Nada, J. Phys. Chem. B **101**, 6167 (1997).
[24] R. R. Gilpin, J. Colloid Interface Sci. **77**, 435 (1980).
[25] G.-J. Kroes, Surf. Sci. **275**, 365 (1992).
[26] J. S. Wettlaufer, Phys. Rev. Lett. **82**, 2516 (1999)
[27] N. J. Harrick, *Internal Reflection Spectroscopy* (Wiley, New York, 1967).
[28] E. O. Palik, *Handbook of Optical Constants of Solids* (Academic, Orlando, 1985).
[29] Z. Zhang and G. E. Ewing, Anal. Chem. (submitted).
[30] M. Born and E. Wolf, *Principles of Optics*, 6th ed. (Cambridge, New York, 1998).
[31] S. G. Warren, Appl. Opt. **23**, 1306 (1984).
[32] H. D. Downing and D. Williams, J. Geophys. Res. **80**, 1656 (1975).
[33] G. C. Pimentel and A. L. McClelland, *The Hydrogen Bond* (Reinhold, New York, 1960).
[34] D. S. Eisenberg and W. Kauzmann, *The Structure and Properties of Liquid Water* (Oxford, New York, 1969).
[35] H. Okumura, T. Akane, and S. Matsumoto, Appl. Surf. Sci. **125**, 125 (1998).
[36] V. Sadtchenko, P. Conrad, and G. E. Ewing, J. Chem. Phys. (in press).
[37] V. Sadtchenko, Z. Zhang, G. E. Ewing, D. Nutt, and A. J. Stone, Langmuir (submitted).
[38] *Natural Research Council (U.S.) International Critical Tables* (McGraw Hill, New York, 1926).
[39] U. Raviv, P. Laurat, and J. Klein, Nature (London) **413**, 51 (2001).
[40] J. P. Devlin, J. Sadley, and V. Buch, J. Phys. Chem. A **105**, 974 (2001).
[41] A. V. Rempel, E. D. Waddington, J. S. Wettlaufer, and M. G. Worster, Nature (London) **411**, 568 (2001).
[42] P. Atkins, *Physical Chemistry*, 6th ed. (Freeman, New York, 1997).
[43] L. A. Wilen, J. C. Wettlaufer, M. Elbaum, and M. Schick, Phys. Rev. B **52**, 12426 (1995).
[44] Y. J. Chabal, Surf. Sci. **168**, 594 (1986).
[45] D. Romanimi, A. A. Kachanov, and F. Stoeckel, Chem. Phys. Lett. **270**, 538 (1997).
[46] S. A. Rice, M. S. Bergren, A. C. Belch, and G. Nielion, J. Phys. Chem. **87**, 4295 (1983).